

# Increasing the hosting capacity of distribution grids by implementing residential PV storage systems and reactive power control

Oscar Camacho Rascon<sup>1,2</sup>

Birgit Schachler<sup>1</sup>, Jochen Bühler<sup>1</sup>

<sup>1</sup> Reiner Lemoine Institute gGmbH  
Berlin, Germany

\*corresponding author: matthias.resch@rl-institut.de

Matthias Resch<sup>1,3,\*</sup>, *Graduate Student Member, IEEE*

Andreas Sumper<sup>3</sup>, *Senior Member, IEEE*

<sup>2</sup> Carl von Ossietzky Universität Oldenburg  
Oldenburg, Germany

<sup>3</sup> UPC - Universitat Politècnica de Catalunya  
Barcelona, Spain

**Abstract**—The rapidly increasing number of implemented photovoltaic (PV) systems in the German distribution grid in recent years has led to power quality issues due to the intermittent generation and reverse power flows in periods of low demand. In order to decrease this impact, different solutions are being investigated. The aim of this study is to analyze the maximum possible grid relief by using residential PV storage systems and different reactive power control strategies from the viewpoint of a distribution system owner. To compare the different voltage control method scenarios the hosting capacity is used as a performance indicator.

**Index Terms**— Distribution grid planning, hosting capacity, residential PV storage, persistence forecast, reactive power control

## I. INTRODUCTION

In Germany, most PV systems are installed in rural grids. In order to avoid over-voltage and equipment over-loading issues in the system traditional grid reinforcement is normally applied. The drawback of this grid planning procedure is the possibly large investment in infrastructure with a low utilization rate. Therefore, technically and economically efficient voltage control strategies that increase the hosting capacity for distributed generation (DG) in distribution grids, as defined in [1], are of major interest. The controllability of DG units (e.g., reactive power provision, active power curtailment) offers alternative ways of voltage control. In order to mitigate curtailment losses due to active power curtailment, residential PV storage systems (RES) with a prognosis based operating strategy are currently promoted in Germany and thoroughly discussed in this paper. The focus of this work is set on autonomously operating voltage control strategies, which rely entirely on locally measured values and need no communication infrastructure.

This paper builds upon previous studies [2] and [3]. In section II a detailed approach for assessing the hosting capacity of LV grids is presented and implemented for an existing distribution grid in Germany. In section III the results

for the aforementioned autonomous voltage control strategies to increase the hosting capacity are discussed and compared. Finally, this work is concluded in Section IV.

## II. METHODOLOGY

This section presents a methodology for directly comparing the technical potential of autonomous reactive power control strategies and residential PV storage systems for increasing a grid's hosting capacity. The methodology is applied to twelve LV grids of a town located in an existing distribution grid in Southern Germany. Its topology, the parameterization of grid elements and used data is described in subsection A. The state of the grid in the year 2014 is used as the baseline. In order to identify the maximum hosting capacity of the grid without any control strategies the PV power is increased according to a PV expansion pathway described in subsection B. This is done by simulating one year in one-minute time steps. This first calculation provides the data of the "current town situation". From the baseline calculation, a period of four consecutive days with the most critical voltage values is identified. Finally, the maximum hosting capacity for these four days is quantified using three control strategies presented. The calculation of the maximum hosting capacity is described in subsection D. For the calculations MATLAB® and MATPOWER [4] are used.

The maximum hosting capacity is reached when limits for over-voltage (OV) at a grid node or over-loading (OL) of equipment are reached. For this study, the voltage related hosting capacity is limited by the permissible voltage band of  $\pm 9\%$  nominal voltage for every minute, to have an additional buffer for measurement accuracy as set in [5]. This is stricter than the current specification for voltage magnitude variations in the DIN EN 50160 where it is stated that for a period of one week the value should not surpass  $\pm 10\%$  of the mean RMS for 95 % of the time during intervals of 10 minutes. The maximal threshold for over-loading is set to 100 % for cables and transformers.

---

This work was supported by the German Federal Ministry of Economics and Technology (BMWi) and the Projektträger Jülich GmbH (PTJ) within the framework of the project "SmartPowerFlow" (FKZ0325523A)

### A. Grid Model

In this paper one MV feeder of the distribution grid is analyzed. The MV feeder is connected to the HV via a 20 kV/110 kV transformer. The slack is located on the HV side of the transformer and its tap ratio is set to reach the voltage of 1.02 p.u. at the MV busbar at the substation. The total length of the MV feeder is 20.2 km and 44 LV grids are connected to it. Twelve of these LV grids form a town which is simulated in detail, whereas the other 32 LV grids are simulated in an aggregated way. The configuration of the grid consists of different elements: loads, generators, lines and transformers. These elements are distributed along the grid on 1208 nodes.

#### 1) Loads

A total of 470 loads are connected to the grid. 441 individual loads are located inside the town and 29 accumulated loads in the surrounding area. Different load profiles are used. To model the consumption behavior three different German standard load profiles in one-minute time steps are used. The distribution of the different profiles is as follows: 264 loads with a H0 household profile, 38 commercial loads with a G0 profile and 35 agricultural loads with a L0 load profile [6]. Additionally, a real heat pump profile from [7] is used in four houses. For the 29 accumulated loads a residential load profile (H0) is used. To dimension the accumulated load a coincidence factor was deduced by analyzing 17 different MV feeders of eleven distribution grids within the grid area of the distribution system operator (DSO). The mean coincidence factor is quantified to be 17 % of the rated power of the MV/ LV transformer apparent power, which matches with the coincidence factor of 15 % assumed in [8]. To adjust the normalized load profiles the measured historical yearly load consumption from 2013 is used in the town. The maximum total yearly consumption of the village is 3.73 GWh. A fix cos $\phi$  of 0.97 is assumed for all loads.

#### 2) Generators

The generated power on this LV grid consists on a group of different type of generators. Along the MV feeder there are 30 aggregated PV systems and 119 residential PV systems (blue roofs in Fig.1) with a total power of 7.7 MVA, four (small) hydro power plants with an aggregated power of 0.51 MVA and one biogas plant of 0.35 MVA. The PV power profile is based on measured data from 2014 and 2013 in one-minute steps connected on a near town (10.1 km). These values were measured at a south oriented system with a nominal power of 107 kW<sub>p</sub>. The normalized PV profile is adjusted by multiplying it with each PV system's nominal power. In order to take into account different orientations, cloud impact etc, a diversity factor, as defined in [9] was taken into account. Based on calculations of [10] it was set to of 85%. If several PV systems are connected to the same PCC for the simulation they were treated as one PV system with the sum of the nominal powers of the single systems. For the hydro generator a normalized load profile was calculated with the aid of generation profiles of several hydro plants located in the south of Germany and published at the EEX Transparency Platform [11]. The biogas plant was set to full power for every time step, according to measured data from an biogas plant in upper Bavaria for the period between 2012 and 2014.

### 3) Lines

The loads, generators and transformers are connected via 1210 lines. For the twelve LV grids of the town the R/X ratio varies between 2.3 (T9) and 5.9 (T7) with a mean value of 3.5. An overview of the three most common line types and lengths for this distribution grid are listed in Table I.

TABLE I. LINE TYPES FOR LV AND MV.

Type	LV (only in town)			MV		
	NAYY	NYN	NAYY	NA2XS2Y		
Diameter [mm <sup>2</sup> ]	70	95	150	150	185	300
Length [km]	5.6	3.7	5.7	10.1	2.1	4.7

### 4) Transformers

Within the town there are 12 MV/LV transformers (20kV / 0.4kV), as depicted in Fig. 1 and listed in Table II. In the surrounding area the remaining 32 LV transformers are connected to the same MV feeder.

TABLE II. TRANSFORMER TYPES FOR LV AND MV.

Rated apparent power of transformer $S_{tr}$ [kVA]											
T1	T2	T3	T4	T5	T6	T7	T8	T9	T10	T11	T12
1E3	160	160	250	160	400	250	160	400	400	400	250

### B. Photovoltaic expansion pathway

In order to assess a hosting capacity for every LV grid (named after their MV/LV transformers T1 to T12), a future PV integration path must be determined. For this purpose, a previous study that established the integration path of PV systems in the town was taken into account [3]. The methodology of [3] was used to estimate the size and location of future PV systems on rooftops using high resolution images to quantify the suitable rooftop surface per building and the appropriate location of the panels. The expansion pathway is determined by the ranking based on the specific yield of the PV system for each LV grid. The pathway is used to increase the number of PV systems and determine the maximum hosting capacity that can be reached using the different reactive control strategies and the residential PV storage system control method. In Fig. 1 the distribution of the future PV systems is marked in orange. In 2012 1.3 MW<sub>p</sub> were installed; the total technical PV potential of the town was calculated to 4.3 MW<sub>p</sub>.

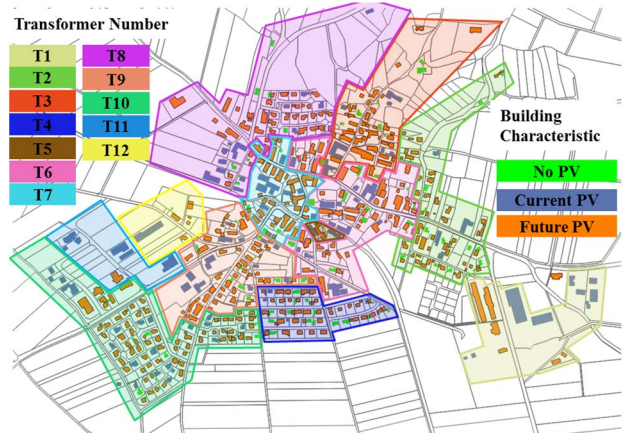


Figure 1. Buildings in the town divided by MV/ LVtransformers (LV-grids) and expansion pathway of PV systems.

### C. Control strategies

Different available options exist to mitigate the voltage raise during periods of reverse power flow. In this work this is done by using the capability of the PV inverter to control reactive power, a so-called  $\cos\phi(P)$  or  $Q(V)$  control, as defined in [12] and [13]. Besides the reactive power control strategies aforementioned, a strategy that mitigates the active power  $P$  by using residential RES is implemented.

#### 1) PV inverter controls

##### a) $\cos\phi(P)$ control

The  $\cos\phi(P)$  control characteristic adjusts the amount of reactive power depending on the active power available in the specific moment as depicted in Fig. 2. When the available active power surpasses 50 % of the PV peak power installed  $P_{PVp}$  in kW the active power will start to reduce at the ratio of a power factor (PF). This is the state of the art reactive power control strategy for PV systems connected to LV in Germany.

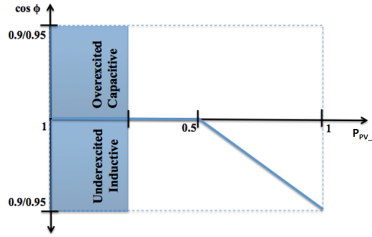


Figure 2. Reactive power curve for  $\cos\phi(P)$ , based on [12].

The PF depends on the size of the nominal PV apparent power  $S_{PVp}$  in kVA, as shown in Table III.

TABLE III. POWER FACTOR CONTROL VALUES DEPENDING ON THE NOMINAL PV APPARENT POWER  $S_{PVp}$ .

$S_{PVp} \leq 13.8 \text{ kVA.}$	$S_{PVp} > 13.8 \text{ kVA.}$
$\cos \phi = 0.95$	$\cos \phi = 0.90$

##### b) $Q(V)$ control

For the  $Q(V)$  control strategy the reactive power is regulated depending on the voltage on the PCC, thus ensuring that the inverter only reacts when reactive power control is required. It is used to reduce line saturation and losses due to an excess of reactive power in the system. The set points of the Q-V curve are still discussed in literature [5], [13], [14]. In this study the Q-V-characteristic was set according to [13] and is depicted in Fig. 3:

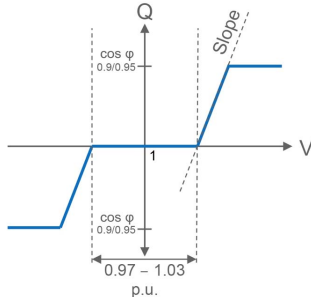


Figure 3. Reactive power curve for  $Q(V)$ .

If the voltage level at the PCC is below 0.97 p.u. or above 1.03 p.u.,  $Q$  injection or absorption is a line with a slope of

11 %, until it reaches the maximum  $Q$  depending on  $P_{PVp}$  as shown in Table III. As previous studies show, the stability of this control type depends highly on the control parameters [14], [15]. Here the stable configuration of [13] is used.

#### 2) PV storage system control

Another type of voltage control strategy is the implementation of RES with feed-in limitation. Since 2013 the increase of self-consumption with RES seems a viable business model for small PV systems in Germany [16]. Nonetheless, the main reasons to invest in RES until 2015 have been ‘soft factors’ such as hedging increasing electricity costs and contributing to the German “Energiewende” [17]. For this reason the German government introduced an incentive program which is also scientifically monitored by [17]. The feed-in limit for the first period of the incentive program was 60 % of  $P_{PVp}$  and will decrease to 50 % for the second period, wherefore the 50 % limit is used in this study. In order to minimize curtailment losses resulting from feed-in limitations different charging methods for RES are being developed. Besides reducing the curtailment loss ratio (CLR), the objective of these control strategies is to increase the self-consumption ratio (SCR) and self-supply ratio (SSR). To compare different control strategies two studies were published: A preliminary review study to compare several control strategies [2] and another to determine the most profitable strategy from the system owner point of view [18] identified the adaptive persistence forecast control strategy as the most profitable one. The methodology of this control strategy is used in this study and presented in detail in [19], [20].

For the purpose of this paper a lithium-ion battery system with a watt-hour efficiency of 95 % and a constant bidirectional battery inverter efficiency of 94 % according to [20] is assumed. This yields a system-round-trip efficiency of 84 %. To assure an optimal performance of the storage system, the usable battery capacity is set between 20% and 90% of its nominal capacity. The battery system capacity  $C$  is sized depending on the nominal PV power  $P_{PVp}$  and the annual load consumption  $LC$  as defined in (1) and (2) and limited to 30 kWh.

$$c = \frac{C [kWh]}{kWh}; p_{PV} = \frac{P_{PVp} [kW_p]}{kW_p}; lc = \frac{LC [MWh]}{MWh} \quad (1)$$

$$c = p_{PV}, \text{ if } p_{PV} \leq lc \text{ and } c = lc, \text{ if } lc \leq p_{PV} \quad (2)$$

#### D. Quantifying the maximum hosting capacity

To calculate the maximum hosting capacity for each LV grid of the town additional PV systems according to the expansion pathway ranking are added one at a time to every LV grid. For each newly added PV system a power flow calculation is conducted in order to check voltages as well as line and transformer loading. PV systems are added until OV or OL occurs for a LV grid. This operation is repeated until all LV grids reach their maximum integration capacity for PV systems. This procedure is used for the three control strategies mentioned in this section and the resulting hosting capacity of all LV grids is compared.



### III. RESULTS

#### A. Validation of the simulated grid model

To validate the simulated grid model the difference between the measured and the simulated active power at the slack is depicted in Fig. 4. This histogram shows the results of a yearly simulation in 1-min steps of the baseline scenario. It can be seen, that the simulated active powers  $P$  are higher than the measured ones, thus showing a more extreme grid state.

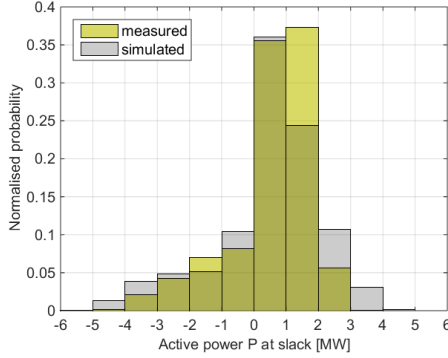


Figure 4. Histogram of  $P$  at the slack.

#### B. Maximum hosting capacity

The baseline scenario is expanded with PV systems until its hosting capacity of 1353 kW<sub>p</sub> for the entire town is reached. This is taken as a reference scenario. The increase in hosting capacity for the three different control strategies to this reference for the whole town as well as for each MV/ LV transformer is presented in Fig. 5.

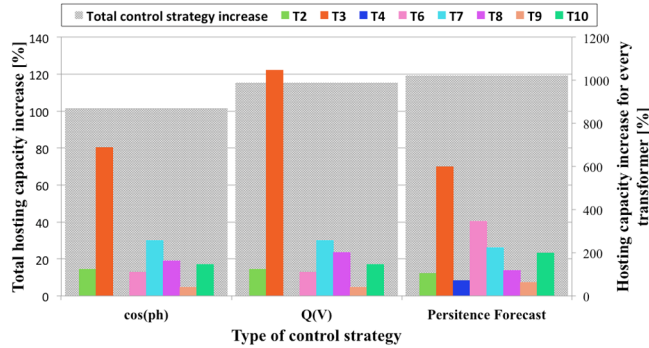


Figure 5. Total hosting capacity for every transformer and control strategy.

A raise of the whole town's PV hosting capacity can be observed for all control strategies. For the  $\cos(\phi)$  control it increases by 101 % (1487 kW), for the  $Q(V)$  control by 116 % (1694 kW) and for RES using a persistence forecast by 119 % (1748 kW). For the different LV grids in the town the gain varies between 0 and 1000 % due to the individual grid topology. For T1, T5, T11 and T12 the hosting capacity limit is not reached and the full potential of the PV expansion pathway can be implemented. If both reactive power control strategies are compared it can be seen that the  $Q(V)$  control leads to a higher PV hosting capacity due to a higher inductive reactive power flow at the slack bus than in the case of a  $\cos(\phi)$  control (Table IV). For the LV grids T2, T4, T6, T7, T9, and T10 the same PV hosting capacity is reached with the  $Q(V)$  and  $\cos(\phi)$  control. A slightly higher hosting capacity is

reached for the grids T3 and T8 with the  $Q(V)$  control as over-voltage can be avoided for all LV grids and the grid capacity can be increased until the thermal limits are reached (see Table V).

TABLE IV. YEARLY SUM OF REACTIVE POWER  $Q$  AT THE SLACK BUS FOR DIFFERENT CONTROL STRATEGIES (LOAD PERSPECTIVE)

Control method	$Q_{ind}$ (inductive)	$Q_{cap}$ (capacitive)
No $Q$ control.	- 5.62 E+3	1.73 E+5
$\cos(\phi)$	- 4.69 E+4	1.66 E+5
$Q(V)$	- 5.93 E+4	1.52 E+5

The causes for reaching the hosting capacity for each LV grid and each control strategy are listed in Table V. The reason can be over-voltage (OV), over-load (OL) or none (OK).

TABLE V. CAUSES FOR REACHING THE HOSTING CAPACITY

Control strategies	LV-grid/ transformer							
	T2	T3	T4	T6	T7	T8	T9	T10
$\cos(\phi)$	OL	OV	OL	OL	OK	OV	OL	OL
$Q(V)$	OL	OL	OL	OL	OK	OL	OL	OL
Persistence forecast	OV	OV	OV	OV	OV	OV	OK	OV

This proves, contrary to what is reported in literature [13], that the amount of reactive power might be higher for the  $Q(V)$  control than for the  $\cos(\phi)$  control, even though the  $Q(V)$  control regulates the reactive power only if the voltage reaches a certain threshold. This is due to the chosen  $Q(V)$ -control characteristic which starts to consume reactive power (load perspective) at 1.03 p.u.. Since the slack bus value is set to 1.02 p.u the  $Q(V)$  control is activated early and reaches its maximum reactive power level when the voltage reaches the value of 1.05 p.u. which is reached very quickly in the LV grids in the case of reverse power flow. Nonetheless, the capacitive reactive power  $Q_{cap}$  needed can be reduced but not in the same magnitude as  $Q_{ind}$  is increased (see Table IV), so that the DSO has to decide if the increased hosting capacity by this control strategy justifies the higher losses. Another option to reduce the losses is to adjust the set points of the  $Q(V)$ -characteristic, as proposed in [5], or lower the voltage at the MV busbar by lowering the set point of the HV/ MV transformer voltage control if possible.

#### C. Active power reduction and losses

As mentioned before, the PV storage systems that were implemented in the LV-grid have the objective to reduce curtailment losses due to the feed-in limitations that are in turn a countermeasure to the increase of PV systems connected to the distribution system. It can be seen from Fig. 5 that in this case the storage systems lead in total to a higher hosting capacity. In contrast to the reactive power control strategies the limiting factor for the active power reduction strategy is OV in all but one LV grid (see Table V). The amount of losses depends on the sizing of the battery. If the sizing methodology presented in section II is applied, the ratio of  $c : p_{PV}$  varies widely wherefore the performance indicators may also vary significantly, as shown in Table VI. In the first case the RES

has a ratio of  $c : p_{PV} : lc$  of 1:53:1, in the second case a ratio of 1:1:8 and in the third case the economically optimal ratio of 1:1:1 [17]. The performance indicators were calculated for the four day period mentioned in section II.

TABLE VI. PERFORMANCE INDICATORS VALUES FOR DIFFERENT BATTERY SIZING CASES.

Case	Performance indicators values to analyze the behavior of different battery sizing cases.		
	SCR	SSR	CLR
$p_{PV} \gg c$	1%	97%	10%
$lc > c$	100%	25%	0%
$p_{PV} = c$	57%	89%	3%

It can be seen that the bigger the difference ratio between load and PV size the poorer the performance of the storage system. In the first case almost all of the load can be covered by the PV system but the curtailment losses are high. In the second case the PV power is consumed completely and no losses occur but the total load cover is modest. In the third case the SCR, SSR and CLR show typical values for an economically optimized system, according to [2]. In order to identify the decrease of curtailment losses through RES a one-year simulation using the maximum hosting capacity for the PV storage systems with persistence forecast control is performed and the amount of curtailed energy with and without storage systems is determined. Without battery systems the total curtailment losses amount to 7.7 % or 4.3 GWh. By implementing the RES using the presented persistence forecast the curtailment losses are decreased by 0.9 %. This slight improvement is due to the fact that only 31 % of the RES are sized within a ratio of  $p_{PV} : lc$  of 0.5:2.

#### IV. CONCLUSION

Two reactive power control strategies ( $\cos(\phi)$  and  $Q(V)$ ) and a prognosis based active power control with RES were evaluated. The control strategies were implemented in a simulation of an existing distribution grid consisting of one MV feeder and several LV-grids. One quarter of the LV-grids were analyzed in detail as they form a town. In order to determine the hosting capacity for each LV-grid PV systems were added according to an expansion pathway. It was shown that under prevailing grid conditions the hosting capacity of the town can be increased by 15 % with the  $Q(V)$  control strategy compared to the  $\cos(\phi)$  control. An 18 % higher integration potential compared to the  $\cos(\phi)$  control is achieved with RES using an active power control. Nevertheless, the active power wasted due to curtailment highly depends on the sizing of the battery which is challenging for the existing PV systems and loads as the dimensions do not ideally match wherefore the sizing of the RES is not optimal. For the chosen sizing method the reduction of curtailed energy is 0.9 %. Future studies could combine reactive and active power control strategies and optimize the non-optimal sizing issue by implementing Community Electricity Storages.

#### ACKNOWLEDGMENT

The authors gratefully acknowledge the contributions of the research group Solar Storage Systems of the HTW Berlin.

#### REFERENCES

- [1] S. Papathanassiou, N. Hatziaargyriou, P. Anagnostopoulos, and L. Aleixo, "Capacity of Distribution Feeders for Hosting DER," *CIGRE Working Group C6.24*. Tech. Rep., p. 149, 2014.
- [2] M. Resch, B. Ramadhani, J. Bühler, and A. Sumper, "Comparison of control strategies of residential PV storage systems," in *9th International Renewable Energy Storage Conference (IRES 2015)*, 2015, p. 18.
- [3] A. Gonzalez Quintairos, J. Bühler, B. Kleinschmitt, and M. Resch, "Analysis of potential distribution and size of photovoltaic systems on rural rooftops," in *GI Forum - Journal for Geographic Information Science*, 2015, pp. 220–224.
- [4] R. D. Zimmerman, C. E. Murillo Sánchez, and R. J. Thomas, "MATPOWER: Steady-State Operations, Planning, and Analysis Tools for Power Systems Research and Education," *Power Syst. IEEE Trans.*, vol. 26, no. 1, pp. 12–19, 2011.
- [5] T. Stetz, K. Diwold, M. Kraiczy, D. Geibel, S. Schmidt, and M. Braun, "Techno-economic assessment of voltage control strategies in low voltage grids," *IEEE Trans. Smart Grid*, vol. 5, no. 4, pp. 2125–2132, 2014.
- [6] C. Fünfgeld and R. Tiedemann, "Anwendung der Repräsentativen VDEW-Lastprofile step by step," *VDEW Mater.*, vol. M-05/2000, p. 34, 2000.
- [7] T. Tjaden, B. Joseph, and V. Quaschnig, "Repräsentative elektrische Lastprofile für Wohngebäude in Deutschland auf 1-sekündiger Datenbasis," *HTW Berlin*. Tech. Rep., p. 8, 2015.
- [8] German Energy Agency (dena), "dena-Verteilnetzstudie. Ausbau- und Innovationsbedarf der Stromverteilnetze in Deutschland bis 2030." Berlin, p. 410, 2012.
- [9] S. Nykamp, "Integrating Renewables in Distribution Grids: Storage, regulation and the interaction of different stakeholders in future grids." Ph.D. dissertation, University of Twente, p. 178, 2013.
- [10] G. Wirth, "Modellierung der Netzeinflüsse von Photovoltaikanlagen unter Verwendung meteorologischer Parameter." Ph.D. dissertation, University Oldenburg, p. 125, 2014.
- [11] European Energy Exchange AG, "EEX Transparency Platform." [Online]. Available: <https://www.eex-transparency.com/>. [Accessed: 23-Feb-2016].
- [12] Verband der Elektrotechnik Elektronik Informationstechnik (VDE), *VDE-AR-N 4105 Generators connected to the low-voltage distribution network*, no. 0105029. 2011, p. 80.
- [13] B. Engel, S. Laudahn, O. Marggraf, and A. Schnettler, "Vergleich von technischer Wirksamkeit sowie Wirtschaftlichkeit zeitnah verfügbarer Verfahren zur Sicherung der statischen Spannungshaltung in Niederspannungsnetzen mit starker dezentraler Einspeisung," *Forum network technology/ network operation in the VDE (FNN)*. Tech. Rep., p. 90, 2014.
- [14] E. Christian, R. Pardatscher, R. Nennung, and R. Witzmann, "Einsatz der Q (U)-Regelung bei der Vorarlberger Energienetze GmbH," *Illwerke und Technische Universität München*. Tech. Rep., p. 110, 2014.
- [15] H. Basse, J. Backes, and T. Leibfried, "Dynamic effect of voltage dependent reactive power control of dispersed generation," in *ETG-Kongress*, 2009, p. 6.
- [16] J. Hoppmann, J. Volland, T. S. Schmidt, and V. H. Hoffmann, "The economic viability of battery storage for residential solar photovoltaic systems - A review and a simulation model," *Renew. Sustain. Energy Rev.*, vol. 39, pp. 1101–1118, 2014.
- [17] K.-P. Kairies, D. Magnor, and D. U. Sauer, "Scientific Measuring and Evaluation Program for Photovoltaic Battery Systems (WMEP PV-Speicher)," *Energy Procedia*, vol. 73, pp. 200–207, Jun. 2015.
- [18] O. Camacho, M. Resch, J. Bühler, B. Schachler, and A. Sumper, "Techno-economic comparison of a schedule based and a forecast based control strategy for residential photovoltaic storage systems in Germany," in *Integration of Sustainable Energy Conference (iSEneC)*, 2016, p. 6.
- [19] J. Bergner, J. Weniger, T. Tjaden, and V. Quaschnig, "Feed-in Power Limitation of Grid-Connected PV Battery Systems with Autonomous Forecast-Based Operation Strategies," in *29th European PV Solar Energy Conference and Exhibition*, 2014.
- [20] J. Weniger, J. Bergner, and V. Quaschnig, "Integration of PV power and load forecasts into the operation of residential PV battery systems," in *4th Solar Integration Workshop*, 2014, pp. 383–390.